Squeezed magnons in an optical lattice: Application to simulation of the dynamical Casimir effect at finite temperature

Xing-Dong Zhao,[1,2] Xu Zhao,[2] Hui Jing,[1,2] Lu Zhou,[2] and Weiping Zhang[2]
[1]*Department of Physics, Henan Normal University, Xinxiang 453007, China*
[2]*Quantum Institute for Light and Atoms, Department of Physics, East China Normal University, Shanghai 200062, China*
(Received 24 November 2012; published 31 May 2013)

We propose to realize controllable squeezing states of ferromagnetic magnons with a spinor Bose-Einstein condensate confined in an optical lattice. We use an external laser field to induce optical dipole-dipole interaction, which leads to magnon excitations of the system. By focusing on the role of the long-range magnetic and the optical dipole-dipole interactions, we show that the existence and properties of the produced squeezed magnons can be well controlled by tuning the transverse trapping widths of the condensates. We also show that the magnon excitations in this system have a close analogy with the dynamical Casimir effect at finite temperature predicted by Plunien *et al*. [Phys. Rev. Lett. **84**, 1882 (2000)] and Jing *et al*. [Phys. Lett. A **268**, 174 (2000)].

DOI: 10.1103/PhysRevA.87.053627 PACS number(s): 03.75.Kk, 42.50.Pq, 32.80.Qk, 37.10.Jk

I. INTRODUCTION

Recent years have witnessed increasing interests about precise measurements and modulations of quantum noise [1–7], which are related to the Heisenberg uncertainty principle [8]. Due to the phase-sensitivity limits set by the inherent uncertainty of quantum systems in the measurement process, people always try to reduce their influence and finally find that, theoretically, the noise can be partially eliminated through quantum squeezing [9]. The achievement of squeezed photons provides possibilities for noiseless optical communication and high-precision measurement [10–16]. In addition to the photon, squeezing states have been realized for diverse kinds of particles over the past few years, such as atoms [17–22], molecules [23–25], and electrons [26–31].

Recently, the squeezing states of quasiparticles also have attracted much attention. An example is a magnon, which can be viewed as a quantized spin wave. Squeezing states of a magnon in ferromagnetic and antiferromagnetic solid spin systems have been studied by tuning the intrinsic parameters of solid materials [32–37], which can not be easily implemented in practice. On the other hand, spinor ultracold atoms in an optical lattice offer a well-controlled platform to study the magnon squeezing state in a ferromagnet. Pu *et al*. have shown that spinor Bose-Einstein condensates (BECs) confined in a one-dimensional deep optical lattice can form an array of coherent atomic spin chains which can undergo a ferromagnetic phase transition [38,39]. The spin waves can be excited and propagate through both long-range magnetic dipole-dipole interaction (MDDI) and optical dipole-dipole interaction (ODDI) [40]. Remarkably, these interactions between atoms can be easily controlled [41,42], where the long-range nonlinear dipole-dipole interactions play a dominant role in resulting spin dynamics. In contrast, they are usually ignored in ordinary condensed matter systems.

Meanwhile, we also note that the dynamical Casimir effect (DCE) describing vacuum radiations created by moving mirrors has received renewed interests in recent years [43–56] . In view of the practical difficulties, many proposals demonstrating the DCE are quite challenging in experiments [51]. Very recently, Wilson *et al*. observed the DCE for the first time by modifying the boundary conditions of an electromagnetic cavity in a superconducting quantum interference device [57]. Since the finite temperature always exists in realistic experiments, many works have focused on the DCE at finite temperature [58–63], including our previous work [64]. In a magnon system, Saito *et al*. studied the magnon excitations in a spinor BEC with a driven external magnetic field and demonstrated an interesting analogy with DCE [65]. The magnon excitations in an atomic spin chain trapped in an optical lattice is similar to that were demonstrated in Ref. [65] for a homogeneous system. However, due to the existence of the MDDI, the process of magnon excitations in our system makes a closer analogy to that of photon excitations in a resonantly vibrating cavity at finite temperature. In this paper, we show that the squeezing states of ferromagnetic magnons can be realized in an optical lattice. In particular, the excited magnons created by the long-range interactions can be used to demonstrate the DCE at finite temperature.

This paper is organized as follows. In Sec. II, we give a conceptual description of spin-wave excitations and magnon in our system. The squeezing and statistical properties of the excited magnons are investigated in detail. In Sec. III, we define the effective temperature (ET) for the excited magnons at initial state, then demonstrate the DCE at finite temperature in this system. In Sec. IV, we present a discussion on detections of the excited magnons and the spin fluctuations, and give a conclusion for this paper in the end.

II. SQUEEZED MAGNON IN AN OPTICAL LATTICE

A. Magnon excitation

As depicted in the top of Fig. 1, we consider $F = 1$ atomic gases trapped in a one-dimensional optical lattice, which is formed by two π-polarized laser beams counterpropagating along the y axis. We assume that the lattice potential is deep enough so that the condensate is divided into a set of separated small condensates equally located at each lattice site. The two lattice laser beams are detuned far from atomic resonance and the condensate confined in the lattice is approximately in its electronic ground state. The laser detuning $\Delta = \omega_L - \omega_a$ (ω_L being laser frequency and ω_a atomic resonant frequency)

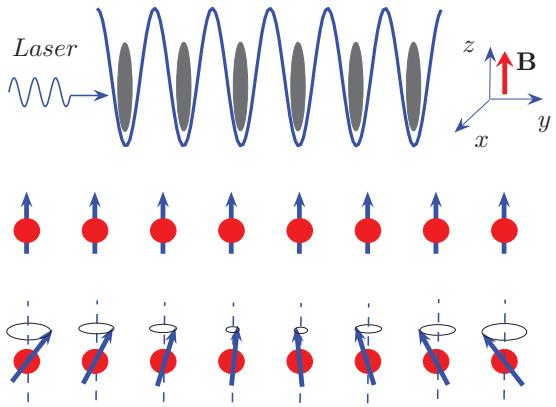

FIG. 1. (Color online) Schematic diagram. Top: spinor BECs polarized by a magnetic field are confined in a one-dimensional optical lattice and an external laser is applied along the y axis. Middle: ferromagnetic ground-state structure of the spinor BEC atomic spin chain. Bottom: spin in each lattice site processes in spin space and spin waves can be excited. The proposed schematic diagram of experiment here has been realized in the previous experiment [as shown in Fig. 1(a) in Ref. [66]].

classifies the optical lattice into two categories: red-detuned optical lattice ($\Delta < 0$) and blue-detuned one $\Delta > 0$. For a blue-detuned lattice we use here, the condensed atoms are trapped at the standing-wave nodes where the laser intensity is approximately zero. As a result, the dipole-dipole interaction induced by lattice beams can be neglected. A strong static magnetic field $\mathbf{B}$ is applied to polarize the ground-state spin orientations of the atomic chain along the quantized z axis [38]. The Hamiltonian takes the following form [67,68]:

$$\begin{aligned} H_M = & \sum_m \int d\mathbf{r} \left\{ \hat{\psi}_m^\dagger \left(-\frac{\hbar^2}{2M}\nabla^2 + V_L \right) \hat{\psi}_m \right\} \\ & + \sum_{m,m',n,n'} \left\{ \int d\mathbf{r} \int d\mathbf{r}' \hat{\psi}_m^\dagger \hat{\psi}_{m'}^\dagger \hat{\psi}_{n'} \hat{\psi}_n V_{mm'n'n}^{\mathrm{col}}(\mathbf{r},\mathbf{r}') \right. \\ & + \frac{1}{2} \int d\mathbf{r} \int d\mathbf{r}' \hat{\psi}_m^\dagger \hat{\psi}_{m'}^\dagger \hat{\psi}_{n'} \hat{\psi}_n V_1(\mathbf{r},\mathbf{r}') \hat{\mathbf{F}}_{mn} \cdot \hat{\mathbf{F}}_{m'n'} \\ & - \frac{1}{2} \int d\mathbf{r} \int d\mathbf{r}' \hat{\psi}_m^\dagger \hat{\psi}_{m'}^\dagger \hat{\psi}_{n'} \hat{\psi}_n V_2(\mathbf{r},\mathbf{r}') \\ & \left. \times \hat{\mathbf{F}}_{mn} \cdot (\mathbf{r}-\mathbf{r}') \hat{\mathbf{F}}_{m'n'} \cdot (\mathbf{r}-\mathbf{r}') \right\}, \\ & + \sum_{m,n} \int d\mathbf{r}\, \hat{\psi}_m^\dagger (-\mu \cdot \mathbf{B})_{mn} \hat{\psi}_n, \end{aligned} \tag{1}$$

where $\hat{\psi}_m(\mathbf{r},t)$ ($m = \pm 1,0$) are the hyperfine ground-state atomic field operators. $V_L(\mathbf{r}) = U_L \exp(-r_\perp^2/W_L^2)\cos^2(k_L y)$ is the light-induced lattice potential, with $r_\perp \equiv \sqrt{x^2+z^2}$, $k_L = 2\pi/\lambda_L$ the wave number, W_L the width of the lattice beams, and the potential depth U_L. $\hat{\mathbf{F}}$ is the total angular momentum operator for the hyperfine spin of an atom, with components represented by 3×3 matrices in the $|f=1, m_f = m\rangle$ subspace. The final term represents the effect of polarizing magnetic field and μ is the magnetic dipole moment.The two-body ground-state collisions and magnetic dipole-dipole interactions are described by the potentials

$$V_{mm'n'n}^{\mathrm{col}}(\mathbf{r},\mathbf{r}') = [\lambda_s \delta_{m'n'}\delta_{mn} + \lambda_a \hat{\mathbf{F}}_{mn} \cdot \hat{\mathbf{F}}_{m'n'}]\delta(\mathbf{r}-\mathbf{r}'), \tag{2}$$

$$V_1(\mathbf{r},\mathbf{r}') = \frac{\mu_0 \gamma_B^2}{4\pi} \frac{1}{|\mathbf{r}-\mathbf{r}'|^3}, \tag{3}$$

$$V_2(\mathbf{r},\mathbf{r}') = \frac{3\mu_0 \gamma_B^2}{4\pi} \frac{1}{|\mathbf{r}-\mathbf{r}'|^5}, \tag{4}$$

where λ_s and λ_a are related to the s-wave scattering length for the spin-dependent interatomic collisions [69]. μ_0 is the vacuum permeability. The parameter $\gamma_B = -\mu_B g_F$ is the gyromagnetic ratio with μ_B being the Bohr magneton and g_F the Landé g factor. Under the single-mode approximation [70], it is convenient to expand the spinor atomic field operator as $\hat{\psi}_m = \sum_i \phi_i(\mathbf{r})\hat{a}_m(i), \phi_i(\mathbf{r})$ is the condensate wave function at the ith lattice site, and $\hat{a}_m(i)$ satisfy the bosonic commutation relations. The spatial wave function of the ith condensate is then determined by the Gross-Pitaevskii (GP) equation

$$\left[-\frac{\hbar^2}{2M}\nabla^2 + V_i(\mathbf{r}) + \lambda_s (N_i - 1)\,|\phi_i(\mathbf{r})|^2 \right] \phi_i(\mathbf{r}) = \mu_i \phi_i(\mathbf{r}), \tag{5}$$

where $V_i(\mathbf{r}) = U_0 \exp(-r_\perp^2/W_L^2)\cos^2(k_L y + i\pi)$ for $0 < y < \lambda_L/2$, $N_i = \sum_m \langle \hat{a}_m^\dagger(i)\hat{a}_m(i)\rangle$ is the number of condensate atoms at the ith site and μ_i is the chemical potential. Here, we define the collective spin operator $\hat{\mathbf{S}}_i = \sum_{mn} \hat{a}_m^\dagger(i)\hat{\mathbf{F}}_{mn}\hat{a}_n(i)$, with components $\hat{S}_i^{\{\pm,z\}}$, $\hat{S}_i^\pm$ are the spin-ladder operators with $\hat{S}_i^\pm = \hat{S}_i^x \pm I\hat{S}_i^y$ ($I^2 = -1$). The Hamiltonian (1) can be rewritten as

$$\begin{aligned} H_M = & \sum_i \left(\lambda_a' \hat{\mathbf{S}}_i^2 - \gamma_B \hat{\mathbf{S}}_i \cdot \mathbf{B} \right) \\ & + \sum_{i,j\neq i} \lambda_{ij} \hat{\mathbf{S}}_i \cdot \hat{\mathbf{S}}_j - \sum_{i,j\neq i} \mathbf{\Lambda}_{ij} : \hat{\mathbf{S}}_i \hat{\mathbf{S}}_j, \end{aligned} \tag{6}$$

where

$$\lambda_a' = (1/2)\lambda_a \int d\mathbf{r} |\phi_i(\mathbf{r})|^4, \tag{7}$$

$$\lambda_{ij} = \frac{1}{2} \int d\mathbf{r} \int d\mathbf{r}' V_1(\mathbf{r},\mathbf{r}') |\phi_i(\mathbf{r})|^2 |\phi_j(\mathbf{r}')|^2, \tag{8}$$

$$\mathbf{\Lambda}_{ij} = \frac{1}{2} \int d\mathbf{r} \int d\mathbf{r}' V_2(\mathbf{r},\mathbf{r}')(\mathbf{r}-\mathbf{r}')(\mathbf{r}-\mathbf{r}') |\phi_i(\mathbf{r})|^2 |\phi_j(\mathbf{r}')|^2. \tag{9}$$

The last term of Eq. (6) is defined as $\mathbf{\Lambda}_{ij} : \hat{\mathbf{S}}_i \hat{\mathbf{S}}_j \equiv \mathbf{\Lambda}_{ij}^\perp (\hat{S}_i^- \hat{S}_j^+ + \hat{S}_i^+ \hat{S}_j^-) + \mathbf{\Lambda}_{ij}^z \hat{S}_i^z \hat{S}_j^z$. The atomic number N_i at each lattice site is small, which reduces the effect of the dipole-dipole interaction. As a result, the dipole-dipole interactions within each site can be safely ignored. In addition, the instability should not be a problem due to the relatively strong strength of s-wave interactions compared to dipole interactions in alkali gases as we used here [71]. For the convenience of calculation, we choose a pancake trap [72], the shape of which can be controlled by tuning the width of external laser field. In this case, we can obtain three important relations for coefficients

in Eqs. (8) and (9):

$$(\mathbf{\Lambda}_{ij})_{xy} = (\mathbf{\Lambda}_{ij})_{xz} = (\mathbf{\Lambda}_{ij})_{zy} = 0, \tag{10}$$

$$(\mathbf{\Lambda}_{ij})_{zz} = (\mathbf{\Lambda}_{ij})_{xx} = (\mathbf{\Lambda}_{ij})^{\perp}, \tag{11}$$

$$(\mathbf{\Lambda}_{ij})_{zz} + (\mathbf{\Lambda}_{ij})_{xx} + (\mathbf{\Lambda}_{ij})_{yy} = 3\lambda_{ij}. \tag{12}$$

Inserting Eqs. (10)–(12) into Hamiltonian (6), finally, we get

$$H_M = \sum_i \left\{ \lambda_a^{'} \hat{\mathbf{S}}_i^2 - \gamma_B \hat{\mathbf{S}}_i \cdot \mathbf{B} - \sum_{j\neq i} J_{ij}^z \left[\hat{S}_i^z \hat{S}_j^z - \frac{1}{2}(\hat{S}_i^- \hat{S}_j^+ + \hat{S}_i^+ \hat{S}_j^-) \right] \right\}, \tag{13}$$

where $J_{ij}^z = \frac{1}{2}[-\lambda_{ij} + (\mathbf{\Lambda}_{ij})_{yy}]$. The coefficient J_{ij} describes the strength of site-to-site spin coupling induced by MDDI, and it has the concrete form [38,40]

$$J_{ij}^z = -\frac{\mu_0 \gamma_B^2}{16\pi\hbar^2} \int d\mathbf{r} \int d\mathbf{r}^{'} \frac{|\mathbf{r}-\mathbf{r}^{'}|^2 - 3|y-y^{'}|^2}{|\mathbf{r}-\mathbf{r}^{'}|^5} \times |\phi_i(\mathbf{r})|^2 |\phi_j(\mathbf{r}^{'})|^2. \tag{14}$$

Obviously, we can see that the dynamics of this system is only dominated by the MDDI, although it has shown rich physics, for instance, spontaneous magnetization, ferromagnetic phase transition, macroscopic spin tunneling, and so on [73–76]. However, because of the large distance, of the order of half of an optical wavelength, between sites, the MDDI is commonly weak so that it is very difficult to induce the observable spin waves. In order to realize the squeezing states of spin waves and demonstrate the dynamical Casimir effect, we need to control the magnetic dipole-dipole interaction. People used to control the magnetic dipole-dipole interactions by tuning the polarized direction of atoms, which can not be used here because the spin directions in the ground state of the system can be changed. So, the atomic ensembles need to be driven by an external laser field. After a laser field with proper optical parameters is applied, the ODDI then will be induced. The ODDI Hamiltonian takes the form

$$H_{\text{opt}} = \sum_{i,j\neq i} J_{ij}^{\text{opt}} (\hat{S}_i^- \hat{S}_j^+ + \hat{S}_i^+ \hat{S}_j^-), \tag{15}$$

where the coefficient J_{ij}^{opt} describing the strength of site-to-site spin coupling induced by the ODDI can be calculated through the integral [38,40]

$$J_{ij}^{\text{opt}} = -\frac{\gamma U_0}{24\Delta\hbar^2 k_L^3} \int d\mathbf{r} \int d\mathbf{r}' f_c(\mathbf{r}-\mathbf{r}') \exp\left(-\frac{r_\perp^2 + r_\perp'^2}{W_L^2}\right) \times \cos(k_L y') \cos(k_L y) \mathbf{e}_{+1} \cdot \mathbf{W}(\mathbf{r}-\mathbf{r}') \cdot \mathbf{e}_{-1} \times |\phi_i(\mathbf{r})|^2 |\phi_j(\mathbf{r}')|^2. \tag{16}$$

In the above integral, the intensity of the external laser is defined as $U_0 = \gamma|\Omega_0|^2/6\Delta_0$, with γ being the spontaneous emission rate of the atoms and Δ_0 the detuning of the applied laser frequency from atomic transition frequency, the time-dependent Rabi frequency $\Omega(t)$ has the form $\Omega(t) = \Omega_0 \sum_i e^{-\frac{(t-i\tau_p)^2}{\tau^2}}$, τ is the pulse duration, and τ_p is pulse interval. The wave number $k_L = 2\pi/\lambda_L$, the transverse coordinate $r_\perp = \sqrt{x^2+z^2}$, and W_L the width of the lattice laser beams. A cutoff function $f_c(\mathbf{r}) = \exp(-r/L_c)$ is introduced to describe the effective interaction range of the ODDI, with L_c being the coherence length. The $\mathbf{e}_{\pm1,0}$ are unit vectors in the spherical harmonic basis. The tensor $\mathbf{W}(\mathbf{r})$ describes the spatial profile of the ODDI and has the form $\mathbf{W}(\mathbf{r}) = \frac{3}{4}[(\mathbf{11} - 3\hat{\mathbf{r}}\hat{\mathbf{r}})(\frac{\sin\xi}{\xi^2} + \frac{\cos\xi}{\xi^3}) - (\mathbf{11} - \hat{\mathbf{r}}\hat{\mathbf{r}})\frac{\cos\xi}{\xi}]$, where $\mathbf{11}$ is the unit tensor, $\hat{\mathbf{r}} = \mathbf{r}/|\mathbf{r}|$, and $\xi = k_L|\mathbf{r}|$. We see that the ODDI in the presently designed optical lattice leads to the spin coupling only in the transverse direction (the direction perpendicular to the magnetic field). On the contrary, the MDDI contributes to spin coupling in both the transverse and longitudinal directions. No matter what the situation is, the atomic spin chain formed in the optical lattice is anisotropic.

Thus, the total Hamiltonian has the form

$$H = H_M + H_{\text{opt}}, \tag{17}$$

where we have ignored both the nonresonant and spin-independent constant terms.

In this paper, we take the ferromagnetic condensates into consideration. In the ground state of the ferromagnetic spin chain of atomic Bose condensates described by Hamiltonian (13), the spins of atoms at each lattice site align up along the direction of the applied magnetic field (the quantized z axis). For a strong magnetic field considered in this paper, the spin deviation from quantized axis is so small that the Hamiltonian can be bosonized in terms of the well-known Holstein-Primakoff transformation for the spin operators (normalized by $\hbar$) [77]:

$$\hat{S}_i^+ = \sqrt{2S}\hat{\varphi}_i \hat{a}_i, \quad \hat{S}_i^- = \sqrt{2S}\hat{a}_i^\dagger \hat{\varphi}_i, \quad \hat{S}_i^z = S - \hat{n}_i, \tag{18}$$

where $\hat{a}_i$ and $\hat{a}_i^\dagger$ are the boson annihilation and creation operator which describe the spin deviation from the quantum z axis, and $\hat{n}_i = \hat{a}_i^\dagger \hat{a}_i$, $\hat{\varphi}_i = (1 - \hat{n}_i/2S)^{1/2}$ with S being the magnitude of spin at site i. Because the spin deviation due to excitations is relatively weak under strong magnetic field, the fourth-order term and other higher-order terms in the expansion of $\hat{\varphi}_i$ can be safely neglected. Thus, Hamiltonian (17) can be transformed into

$$H = H_0 + H_1 + H_2, \tag{19}$$

$$H_0 = E_0 + \gamma_B B_z \sum_i \hat{a}_i^\dagger \hat{a}_i, \tag{20}$$

$$H_1 = \frac{1}{2} \sum_{i,j\neq i} [-2J_{ij}^z \hat{a}_i^\dagger \hat{a}_j^\dagger \hat{a}_i \hat{a}_j + J_{ij}(\hat{a}_j^\dagger \hat{a}_j^\dagger \hat{a}_j \hat{a}_i + \hat{a}_i^\dagger \hat{a}_i^\dagger \hat{a}_i \hat{a}_j + \hat{a}_j^\dagger \hat{a}_i^\dagger \hat{a}_i \hat{a}_i + \hat{a}_i^\dagger \hat{a}_j^\dagger \hat{a}_j \hat{a}_j)], \tag{21}$$

$$H_2 = S \sum_{i,j\neq i} [J_{ij}^z (\hat{a}_i^\dagger \hat{a}_i + \hat{a}_j^\dagger \hat{a}_j) - 2J_{ij}(\hat{a}_i^\dagger \hat{a}_j + \hat{a}_j^\dagger \hat{a}_i)], \tag{22}$$

where $E_0 = \lambda_a^{'} MS(S+1) - \gamma_B B_z MS - \sum_{i,j\neq i} J_{ij}^z S^2$, with M being the total number of lattice sites. The interaction coefficient J_{ij} satisfies $J_{ij} = J_{ij}^{\text{opt}} - \frac{1}{2}J_{ij}^z$. The Hamiltonian (19) describes the excitations of nonlinear spin waves in the ferromagnetic spin chain of atomic spinor BECs. Here, we are interested in how to realize the squeezing states of magnons in this system; in order to achieve it, we need to further introduce the Fourier transformation to the operators

$\hat{a}_m$ and $\hat{a}_m^\dagger$:

$$\hat{a}_{\mathbf{k}} = \frac{1}{\sqrt{M}} \sum_i e^{I\mathbf{k}\cdot\mathbf{R}_i} \hat{a}_i, \tag{23}$$

$$\hat{a}_{\mathbf{k}}^\dagger = \frac{1}{\sqrt{M}} \sum_i e^{-I\mathbf{k}\cdot\mathbf{R}_i} \hat{a}_i^\dagger, \tag{24}$$

where $\mathbf{R}_i$ is the position of the ith lattice site. Insert Eqs. (23) and (24) into (19), with the help of the relation $\frac{1}{M}\sum_i \exp[I(\mathbf{k}-\mathbf{k}')\cdot\mathbf{R}_i] = \delta_{\mathbf{k}\mathbf{k}'}$, theHamiltonian (19) can be expressed in terms of creation and annihilation operators $\hat{a}_{\mathbf{k}}^\dagger$ and $\hat{a}_{\mathbf{k}}$ in wave-vector space. After ignoring the constant terms, we get the effective Hamiltonian

$$H = \sum_{\mathbf{k}} \omega_{\mathbf{k}} \hat{a}_{\mathbf{k}}^\dagger \hat{a}_{\mathbf{k}} + \sum_{\mathbf{k},\mathbf{k}',\mathbf{q}} V_{\mathbf{k},\mathbf{k}',\mathbf{q}} \hat{a}_{\mathbf{k}-\mathbf{q}}^\dagger \hat{a}_{\mathbf{k}'+\mathbf{q}}^\dagger \hat{a}_{\mathbf{k}'} \hat{a}_{\mathbf{k}}, \tag{25}$$

where $\omega_{\mathbf{k}} = \gamma_B B_z + 2S\sum_{i\neq 1} J_{1i}^z - 4SJ_{\mathbf{k}}$ is the frequency of the magnon with wave vector $\mathbf{k}$. The last term of Hamiltonian (25) describes the momentum-conserved nonlinear magnon-magnon interactions, and it can be explained by the following process: two magnons with wave vector $\mathbf{k}, \mathbf{k}'$ are annihilated, at the same time two magnons $\mathbf{k}-\mathbf{q}$, $\mathbf{k}'+\mathbf{q}$ are created or one magnon transfers momentum $\mathbf{q}$ to another. The interaction matrix element $V_{\mathbf{k},\mathbf{k}',\mathbf{q}}$ has the form

$$V_{\mathbf{k},\mathbf{k}',\mathbf{q}} = -\frac{1}{M}\left[J_{\mathbf{k}'+\mathbf{q}-\mathbf{k}}^z - (J_{\mathbf{k}} + J_{\mathbf{k}-\mathbf{q}})\right], \tag{26}$$

where

$$J_{\mathbf{k}}^z = \sum_{i\neq 1} J_{i1}^z \exp\left[I\mathbf{k}\cdot(\mathbf{R}_1 - \mathbf{R}_i)\right], \tag{27}$$

$$J_{\mathbf{k}} = \sum_{i\neq 1} J_{i1} \exp\left[I\mathbf{k}\cdot(\mathbf{R}_1 - \mathbf{R}_i)\right] \tag{28}$$

are Fourier transformations of the longitudinal and the transverse dipole-dipole interactions. Since the total momentum of magnon system is zero, the magnons of opposite wave vectors will always appear simultaneously. In the standing-wave configuration, a magnon pair is stable only if the two magnons have opposite wave vectors $\mathbf{k}$ and $-\mathbf{k}$ [32]. By using a mean-field technique, we get a more simplified effective pair-excitation Hamiltonian

$$H = \sum_{k>0} [\omega'_{\mathbf{k}}(\hat{a}_{\mathbf{k}}^\dagger \hat{a}_{\mathbf{k}} + \hat{a}_{-\mathbf{k}}^\dagger \hat{a}_{-\mathbf{k}}) + \chi_{\mathbf{k}}(\hat{a}_{\mathbf{k}}^\dagger \hat{a}_{-\mathbf{k}}^\dagger + \text{H.c.})] \tag{29}$$

and

$$\omega'_{\mathbf{k}} = 4S(J_0 - J_{\mathbf{k}}) + \frac{2N_0}{M}\left(2J_{\mathbf{k}} - J_{\mathbf{k}}^z\right), \tag{30}$$

$$\chi_{\mathbf{k}} = \frac{2N_0}{M}\left(J_0 + J_{\mathbf{k}} - J_{\mathbf{k}}^z\right), \tag{31}$$

where N_0 is the number of magnons with $\mathbf{k} = \mathbf{0}$. So far, we have obtained a squeezed Hamiltonian consisting of two-mode squeezed components. At the initial time, we prepare the initial state under the condition that the external driven laser does not exist. There are two aspects needed to be taken into account: First, it must be more convenient to control the MDDI alone than to control both the MDDI and the ODDI simultaneously while we are preparing the initial states; second, after the initial state is prepared, the external laser applied can play the role of the driving field in demonstrating the dynamic Casimir effect. In order to obtain the dynamical properties of excitations and the number of excited magnons, we need to calculate the wave function of the system at arbitrary time. We diagonalize the effective Hamiltonian (29) via Bogoliubov transformation [78]

$$\hat{c}_{\mathbf{k}} = \hat{a}_{\mathbf{k}} \cosh\gamma_{\mathbf{k}} + \hat{a}_{-\mathbf{k}}^\dagger \sinh\gamma_{\mathbf{k}}, \tag{32}$$

$$\hat{c}_{\mathbf{k}}^\dagger = \hat{a}_{\mathbf{k}}^\dagger \cosh\gamma_{\mathbf{k}} + \hat{a}_{-\mathbf{k}} \sinh\gamma_{\mathbf{k}}, \tag{33}$$

with parameter $\gamma_{\mathbf{k}} = \frac{1}{2}\text{arc}\tanh(\chi_{\mathbf{k}}/\omega_{\mathbf{k}})$ determined by the MDDI. As introduced in Refs. [32,33], we choose the initial state as

$$|\Psi(0)\rangle = \prod_{k>0} \exp[\gamma_{\mathbf{k}}(\hat{a}_{-\mathbf{k}}\hat{a}_{\mathbf{k}} - \hat{a}_{\mathbf{k}}^\dagger \hat{a}_{-\mathbf{k}}^\dagger)]|0_{\mathbf{k}}, 0_{-\mathbf{k}}\rangle, \tag{34}$$

where the unitary transformation $\exp[\gamma_{\mathbf{k}}(\hat{a}_{-\mathbf{k}}\hat{a}_{\mathbf{k}} - \hat{a}_{\mathbf{k}}^\dagger \hat{a}_{-\mathbf{k}}^\dagger)]$ is a two-mode squeezing operator [79,80], with $\gamma_{\mathbf{k}}$ the squeezing factor. $|0_{\mathbf{k}}, 0_{-\mathbf{k}}\rangle$ denotes a two-mode magnon vacuum state, and $\hat{c}_{\mathbf{k}}|\Psi(0)\rangle = 0$. In this case, the number of the excited magnons in wave-vector space has expectation value

$$N_M(\mathbf{k}) = \langle\Psi(0)|\hat{a}_{\mathbf{k}}^\dagger \hat{a}_{\mathbf{k}}|\Psi(0)\rangle = \sinh^2\gamma_{\mathbf{k}}. \tag{35}$$

In our calculations, we consider the discrete momentum satisfying $\mathbf{k}\cdot\mathbf{R}_i = 2\pi l/M$; here l is an integer. Obviously, by tuning the MDDI we can prepare different initial states, which initiates the possibility of demonstrating DCE at finite temperature.

After the initial state is prepared, we apply an external laser to drive the system, which can induce the ODDI and produce new excitations subsequently. In the Schrödinger representation, the state of the excited magnons with MDDI and ODDI at an arbitrary time t can be expressed as

$$|\Psi(t)\rangle = \prod_{k>0} \{\exp[-I\omega_{\mathbf{k}} t(\hat{a}_{\mathbf{k}}^\dagger \hat{a}_{\mathbf{k}} + \hat{a}_{-\mathbf{k}}^\dagger \hat{a}_{-\mathbf{k}})] \times \hat{S}(\xi_{\mathbf{k}})\hat{S}(\gamma_{\mathbf{k}})|0_{\mathbf{k}}, 0_{-\mathbf{k}}\rangle\}, \tag{36}$$

where the second squeezing operator $\hat{S}(\xi_{\mathbf{k}})$ takes the form [79,80]

$$\hat{S}(\xi_{\mathbf{k}}) = \exp(\xi_{\mathbf{k}}^* \hat{a}_{-\mathbf{k}}\hat{a}_{\mathbf{k}} - \xi_{\mathbf{k}}\hat{a}_{\mathbf{k}}^\dagger \hat{a}_{-\mathbf{k}}^\dagger), \tag{37}$$

with $\xi_{\mathbf{k}} = I\lambda_{\mathbf{k}} e^{I\omega_{\mathbf{k}}t}$, $\lambda_{\mathbf{k}} = \frac{\chi_{\mathbf{k}}}{\omega_{\mathbf{k}}}|\sin\omega_{\mathbf{k}}t|$. From Eq. (36), the number of excited magnons with wave number $\mathbf{k}$ can be obtained as

$$N_{\mathbf{k}}(t) = \sinh^2\gamma_{\mathbf{k}} + \sinh^2\lambda_{\mathbf{k}} + 2\sinh^2\gamma_{\mathbf{k}}\sinh^2\lambda_{\mathbf{k}} - \tfrac{1}{2}\sinh(2\lambda_{\mathbf{k}})\sinh(2\gamma_{\mathbf{k}})|\sin(\omega_{\mathbf{k}}t)|. \tag{38}$$

In the right-hand side of Eq. (38), the first term describes the number of magnons produced by the MDDI; the second term shows the number of magnons created by the ODDI; the last two terms stand for the interference effect induced by both two dipole-dipole interactions. If the sum of the last two terms is negative, it is expected to cause a destructive interference effect; otherwise, it will present a constructive interference effect.

B. Squeezing properties

In fact, the squeezing state of magnon was first studied in an antiferromagnet, where the fluctuation of the spin component

may satisfy the requirement of generating the magnon squeezing states due to the interference between two sublattice spin waves. Because of the uniform spin orientations, its generating mechanism is obviously not suitable for the ferromagnet case, so people are likely to focus more and more attention on how to generate a squeezing state in a ferromagnet. In solid material, it has been theoretically proposed that the squeezing state of magnon in a ferromagnet could be generated by using the nonlinear interactions between magnons with different energy [32,33]. According to the above analysis, the magnons in the spin chain can be excited by two different channels (the ODDI and the MDDI) and the excited magnons may interact with each other; furthermore, their interactions can be well controlled. It is very convenient for us to study the possibility of achieving squeezing states in a ferromagnet. In order to find out the condition of achieving the squeezing state of magnons, we need to calculate the quantum fluctuation of spin component $\hat{S}_x$ (or $\hat{S}_y$). For $\hat{S}_x$, the spin fluctuation is defined as

$$\left\langle \Delta \hat{S}_x^2 \right\rangle = \left\langle \hat{S}_x^2 \right\rangle - \langle \hat{S}_x \rangle^2, \tag{39}$$

where $\langle \ldots \rangle$ stands for the expectation value of a certain operator in the state $|\Psi(t)\rangle$. The expectation value of the x component of total spins is zero for this system. However, the fluctuation of the x-axis component of spins can be expressed as

$$\left\langle \Delta S_x^2 \right\rangle = S \sum_{\mathbf{k}} \sum_i e^{-I\mathbf{k}\cdot\mathbf{R}_i} \left[1 + 2\,\mathrm{Re}\,\langle \hat{a}_{\mathbf{k}} \hat{a}_{-\mathbf{k}} \rangle + 2N_{\mathbf{k}}(t) \right], \tag{40}$$

where

$$\begin{aligned} \mathrm{Re}\langle \hat{a}_{\mathbf{k}} \hat{a}_{-\mathbf{k}} \rangle &= \sinh(2\gamma_{\mathbf{k}}) \cosh^2 \lambda_{\mathbf{k}} \sin^2(\omega_{\mathbf{k}} t) - \tfrac{1}{2} \sinh(2\gamma_{\mathbf{k}}) \\ &\quad - \tfrac{1}{2} \sinh(2\lambda_{\mathbf{k}}) \cosh(2\gamma_{\mathbf{k}}) |\sin(\omega_{\mathbf{k}} t)|. \end{aligned} \tag{41}$$

Equation (40) has made a link between the number of excited magnons and spin fluctuations. Remarkably, it should be interesting to study the relation between the spin fluctuations and the number fluctuations, which will draw our attention in future work. We denote $G_{\mathbf{k}}(t) = S[1 + 2\,\mathrm{Re}\,\langle \hat{a}_{\mathbf{k}} \hat{a}_{-\mathbf{k}} \rangle + 2N_{\mathbf{k}}(t)]$ as the fluctuation of $\hat{S}_x$ in the $\mathbf{k}$ space, and the $G_{\mathbf{k}}(0)$ is the fluctuation of the vacuum states. When $G_{\mathbf{k}}(t)$ is less than the $G_{\mathbf{k}}(0)$ in some time regions, the magnon system is in the squeezing states. We can therefore define the squeezing criterion of the magnon as

$$\begin{aligned} F_{\mathbf{k}}(t) &= [G_{\mathbf{k}}(t) - G_{\mathbf{k}}(0)]/S \\ &= 2\sinh(2\gamma_{\mathbf{k}}) \cosh^2 \lambda_{\mathbf{k}} \sin^2(\omega_{\mathbf{k}} t) + \cosh(2\gamma_{\mathbf{k}}) \cosh(2\lambda_{\mathbf{k}}) \\ &\quad - \sinh(2\lambda_{\mathbf{k}}) |\sin(\omega_{\mathbf{k}} t)| e^{2\gamma_{\mathbf{k}}} - \sinh(2\gamma_{\mathbf{k}}) < 0. \end{aligned} \tag{42}$$

In our previous works, we have demonstrated that the MDDI and the ODDI can be well controlled by tuning the transverse trapping width w of the condensate [41,42]; here, we still use this method to tune the dipole-dipole interactions. In Fig. 2, it is shown that the magnon squeezing states occur with appropriate system parameters. By observing that the ODDI and MDDI decrease rapidly with the increase of the transverse trapping width of the condensate, we choose three different transverse trapping widths: $w = 1.5\lambda_L$, $1.98\lambda_L$, and $3.0\lambda_L$, respectively. These regions in which the values of $F_{\mathbf{k}}(t)$ are less than zero satisfy the condition of achieving a magnon squeezing state, otherwise the squeezing states do not exist. Obviously, a magnon squeezing state can not be obtained if larger transverse trapping widths are chosen (the dotted black and dashed blue lines), and the ODDI is weaker in this case. Contrarily, when a smaller transverse trapping width is selected to enhance the site-to-site couplings, it shows that we can realize the magnon squeezing state in this system (the solid red line).

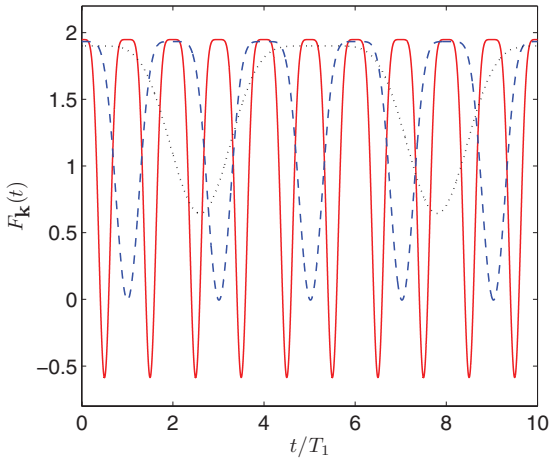

FIG. 2. (Color online) Schematic representation of magnon squeezing. We choose three transverse trapping widths of the condensate: $w = 1.5\lambda_L$ (solid red line), $1.98\lambda_L$ (dashed blue line), and $3.0\lambda_L$ (dotted black line), respectively. Time unit $T_1 = 2\pi/\omega_{\mathbf{k}}$ is the period of the $k = 1$ (in units of $k_0 = 2k_L/M$) mode for $w = 1.5\lambda_L$. The gyromagnetic ratio is chosen as $\gamma_B = -\mu_B/2$ of the electronic ground state of ^{87}Rb. The strength of the external laser is taken as $\gamma\,|\Omega_0|^2/\Delta_0^2 = 10^3$. We have taken $\lambda_L = 1\ \mu$m and used a total number of 100 lattice sites with 2000 atoms in each site.

Further studies show that there is a critical value of the transverse trapping width w for this system to achieve a magnon squeezing state $w_c = 1.98\lambda_L$. As the transverse trapping width is reduced below the critical value w_c, the MDDI and the ODDI become stronger and they will induce squeezing states in the ferromagnetic magnons. In addition, we find that the squeezing regions appear periodically and the period depends on the long-range dipole-dipole interactions. This paper aims to not only create the squeezing states of magnons on one hand, but also study their characteristics and applications on the other hand; therefore, we will first focus on the statistical properties of the produced magnons.

C. Statistical properties

In an ordinary optical system, the importance of statistical properties of photons lies not only in their academic sense but also in their practical applications. In what follows, we will show the similarities between photons in an optical cavity system and the excited magnons in an atomic spin chain in the optical lattice and find applications for the excited magnons in our system. In this sense, it is important for us to study the statistical properties of magnons if we want to get a thorough understanding of the magnons and make use of them. To find the statistical properties of the excited magnons, we introduce

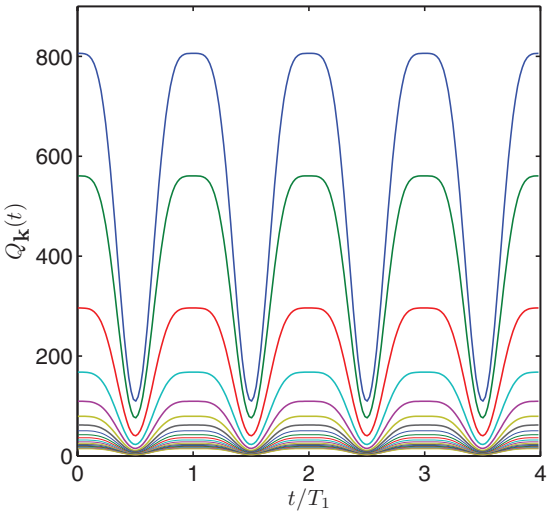

FIG. 3. (Color online) Plot the Mandel factor $Q_{\mathbf{k}}$ versus time t for the principal mode $k = 1$ under different transverse trapping widths w of the condensate. Lines from the top to the bottom correspond to $w = 0.1\lambda_L \sim 30\lambda_L$. Time unit ($T_1 = 2\pi/\omega_{\mathbf{k}}$) is the rescaled period of the $k = 1$ mode for each w. The other parameters are chosen the same as in Fig. 2.

a Mandel factor [81]

$$Q_{\mathbf{k}}(t) = \frac{\langle[\Delta N_{\mathbf{k}}(t)]^2\rangle}{\langle N_{\mathbf{k}}(t)\rangle} - 1, \tag{43}$$

which can be used to measure the deviation from Poisson distribution, and thus to distinguish the quantum process from the classical one. In our system, we have

$$\begin{aligned}\left\langle N_{\mathbf{k}}^2(t)\right\rangle = {} & \tfrac{1}{4}[a^2 + c^2 + (b^2 + d^2)\sinh^2\gamma_{\mathbf{k}}\cosh(2\gamma_{\mathbf{k}}) \\ & + 2(ab + cd)\sinh^2\gamma_{\mathbf{k}}],\end{aligned} \tag{44}$$

where

$$\begin{aligned} a &= 2\sinh^2\lambda_{\mathbf{k}} + \sinh(2\lambda_{\mathbf{k}})\tanh\gamma_{\mathbf{k}}\cos\theta, \\ b &= 2\cosh(2\lambda_{\mathbf{k}}) + 2\sinh(2\lambda_{\mathbf{k}})\tanh^{-1}(2\gamma_{\mathbf{k}})\cos\theta, \\ c &= \sinh(2\lambda_{\mathbf{k}})\tanh\gamma_{\mathbf{k}}\sin\theta, \\ d &= 2\sinh(2\lambda_{\mathbf{k}})\sinh^{-1}(2\gamma_{\mathbf{k}})\sin\theta \end{aligned} \tag{45}$$

and $\theta = \pi/2 + \omega_{\mathbf{k}}t$. Combining Eqs. (38) with (44), we can calculate $Q_{\mathbf{k}}(t)$ at an arbitrary time. In Fig. 3, numerical analyses of $Q_{\mathbf{k}}$ for w in the range of ($0.1\lambda_L \sim 30\lambda_L$) show that the Mandel factor is always positive, i.e., $Q_{\mathbf{k}} > 0$, no matter which parameters are chosen. In other words, the magnons excited by the ODDI and the MDDI in the optical lattice obey super-Poisson statistical distribution, and the variance of the number of magnons would have to be greater than the mean. Similarly, we can investigate the other characteristics of the excited magnons, which depend on their applications.

III. DEMONSTRATE THE DYNAMICAL CASIMIR EFFECT AT FINITE TEMPERATURE

A. Effective temperature representation for magnon excitations

At initial time, the spinor BECs are loaded into the blue-detuned optical lattice, so there is no ODDI induced and the spin coupling is governed only by the coefficient J_{lj}^z from the static magnetic dipole-dipole interaction. In this case, a small amount of magnons can be excited though the weak MDDI, and their number can be controlled as shown in Eq. (35). By introducing effective temperature of this system, we are likely to make a quantitative analysis of the effect of the initial value in the whole excitation process.

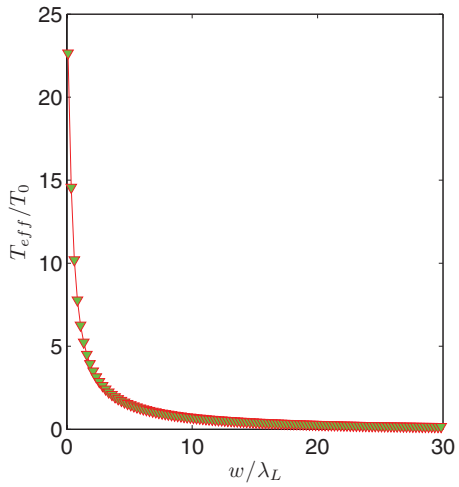

FIG. 4. (Color online) Scaled effective temperature T_{eff}/T_0 versus the transverse trapping width w of the condensate. Here, $T_0 = 6.116 \times 10^{-7}$ K, the other parameters are chosen the same as in Fig. 2.

It has been theoretically [82] and experimentally [83] confirmed that magnons behave like bosons. So, the excited magnons here obey the Bose-Einstein statistics [84], that is, $f(E_{\mathbf{k}}) = \frac{1}{\exp(E_{\mathbf{k}}/k_B T_{\text{eff}})-1}$ approximately, where $E_{\mathbf{k}}$ is the energy of the kth mode, k_B is the Boltzmann constant, and T_{eff} is an effective temperature defined for the excited magnons, namely,

$$T_{\text{eff}} = \frac{\hbar\omega_{\mathbf{k}}}{k_B}\ln^{-1}(\eta_+/\eta_-), \tag{46}$$

with $\eta_\pm = \omega_{\mathbf{k}} \pm \sqrt{\omega_{\mathbf{k}}^2 - \chi_{\mathbf{k}}^2}$. In Fig. 4, we plot T_{eff} versus the transverse width w. It shows that T_{eff} drops rapidly with the increase of the parameter w and it tends to zero for large w. This is perfectly consistent with the results on the modulational instability of nonlinear coherent spin waves in this system got from our previous works, in which we found that the spin-wave modes with small $\mathbf{k}$ become more stable as the transverse width w increases. In other words, it is difficult for us to obtain a large number of excitations for the long-wavelength spin waves $\mathbf{k} \approx 0$ when larger w is chosen, so the effective temperature chosen must be lower in this case. By tuning the transverse width, we can prepare the initial states with the magnon population distributions at different ET. They are similar to the initial photons in the optical cavity dynamical Casimir effect at finite temperature, which provides a unique tool for us to study the DCE at finite temperature.

B. Dynamical Casimir effect at finite effective temperature

In order to demonstrate the DCE at finite effective temperature in this magnon system, we first need to review the DCE for an electromagnetic field in a resonantly vibrating cavity. In general, the expectation values of the electric and magnetic

fields are zero: $\langle\hat{\mathbf{E}}(\mathbf{r},0)\rangle = \langle\hat{\mathbf{H}}(\mathbf{r},0)\rangle = 0$ in the initial state, and they satisfy the Heisenberg equations of motion [65]

$$\frac{\partial}{\partial t}\varepsilon(\mathbf{r},t)\hat{\mathbf{E}}(\mathbf{r},t) = \nabla \times \hat{\mathbf{H}}(\mathbf{r},t), \tag{47}$$

$$\frac{\partial}{\partial t}\hat{\mathbf{H}}(\mathbf{r},t) = -\nabla \times \varepsilon(\mathbf{r},t)\hat{\mathbf{E}}(\mathbf{r},t), \tag{48}$$

where $\varepsilon(\mathbf{r},t)$ is the dielectric constant. From Eqs. (47) and (48), we can see that the expectation values of the electric and magnetic fields remain zero, i.e., $\langle\hat{\mathbf{E}}(\mathbf{r},t)\rangle \equiv \langle\hat{\mathbf{H}}(\mathbf{r},t)\rangle \equiv 0$. However, the vacuum fluctuation of electromagnetic field can be amplified and photons are excited at the same time. The suitable condition for studying the DCE is that the quantum fluctuation is excited and the expectation values of the relevant quantum fields remain constant during the temporal variation of the external parameters [65]. The present system is suitable for investigating the DCE since $\langle\hat{S}_x\rangle = \langle\hat{S}_y\rangle = 0$ holds while the external laser is applied to drive the system and new magnons are excited. Furthermore, as introduced in Sec. III A, the MDDI can induce a controllable initial excitation described by the finite ET, considering that, we could easily study the DCE at a finite temperature.

We have studied the DCE at finite temperature by using the approach of thermal field theory in our previous work [64]. Here, we will draw a link between the magnon excitations in the atomic spin chain and the phonon excitations in a vibrating cavity at nonzero temperature from different perspectives. For the latter, in the initial state the creation rate of photons depends on the cavity temperature, and these photons of the thermal vacuum obey the Bose-Einstein distribution. It corresponds to the initial magnons in the atomic spin chain which only depend on the MDDI. As the cavity is vibrating, new photons are excited in the thermodynamical process and the number of photons is related to both the temperature of the cavity and the motion of the mirror; analogously, the new excited magnons depend on both the MDDI and the ODDI in our system after the external laser is applied. In the optical vibrating cavity, the number of creative photons will be three orders of magnitude larger than that of the pure vacuum case, which is just the strong enhancement effect or avalanche effect; this feature is important for us to distinguish the DCE from a general enhancement effect.

In our system, we turn on the driving laser rapidly after the initial states are prepared; the time evolution of the compounded excitations $N_{\mathbf{k}}(t)$ is shown in Fig. 5. Here, we choose two marked values of the transverse trapping width w ($0.1\lambda_L$ and $20\lambda_L$ as shown in Fig. 4). In Fig. 5(a), we take $w = 0.1\lambda_L$, which corresponds to a higher ET. We can see clearly that some magnons with $k > 1$ are produced in the process of evolution. Contrarily, it shows that the number $N_{\mathbf{k}}(t)$ only takes on a periodically oscillating behavior for a few principal modes, and magnons for larger k can be hardly excited when we take $w = 20\lambda_L$, which corresponds to a lower ET case as shown in Fig. 5(b). In other words, although they share the same external laser, the ultimate excitations are obviously different from each other, especially, the number of magnons excited by ODDI is evidently limited for a low-temperature case. This means that the initial values play an important role in excitations of magnon in this system.

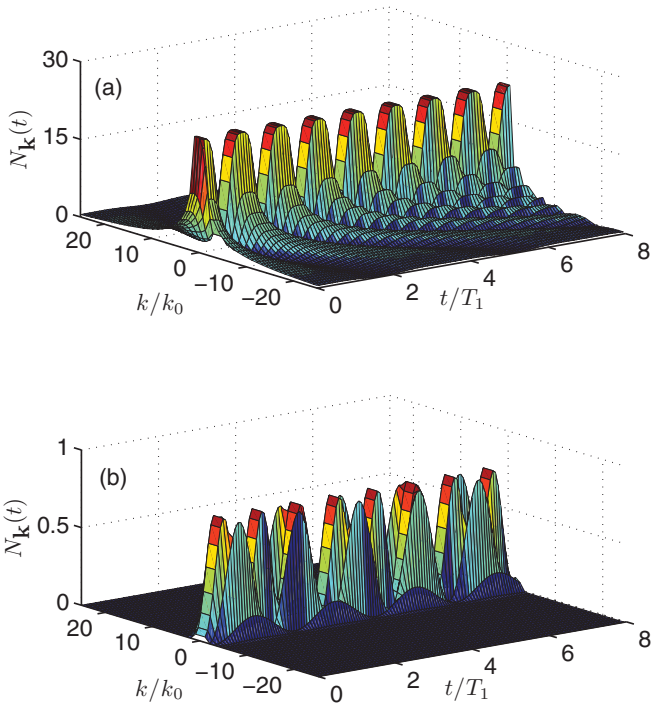

FIG. 5. (Color online) Plot $N_{\mathbf{k}}(t)$ versus k and t for two extreme values of w shown in Fig. 2. For (a) $w = 0.1\lambda_L$ (the higher ET case), and (b) $w = 20\lambda_L$ (the lower ET case). The other parameters are chosen the same as in Fig. 2.

In order to observe the enhancement effect, we define $\bar{N}$ as the mean number of the excited magnons

$$\bar{N}(T) = \frac{1}{T}\sum_{\mathbf{k}}\int_0^T N_{\mathbf{k}}(t)dt. \tag{49}$$

For comparison, we also calculate the mean number of the excited magnons from the pure vacuum defined as $\bar{N}_0$, and we show the magnification factor of the mean number of the excited magnons in Fig. 6. From Eq. (16), we can see that the strength of the ODDI can be controlled by tuning the the intensity of the external laser, thus three different values of the external laser intensity are selected. It is obvious that the magnification factor grows with the increase of the ET once the other parameters are fixed, and the mean number of excited magnons will be three orders of magnitude larger than the pure vacuum case when the proper parameter is chosen as shown in Fig. 6 by solid circles. It is worth emphasizing that the stronger laser does not necessarily mean larger amplification factor, on the contrary, the amplification factors are smaller when the external laser is strong enough as shown in Fig. 6 by triangles. Our numerical calculations show that we can get a large amplification factor only when the ODDI is accurately controlled. From analytical analysis, the number of magnons is dominated by two squeezing operators, i.e., $\hat{S}(\xi_{\mathbf{k}})\,\hat{S}(\gamma_{\mathbf{k}})$, as we can see from Eq. (36). Tuning the system parameters means changing the exponents of two operators, consequently, the number fluctuation will be enhanced once the two operators satisfy a special phase-matching condition. From a physical point of view, the two mechanisms (magnetic and light-induced

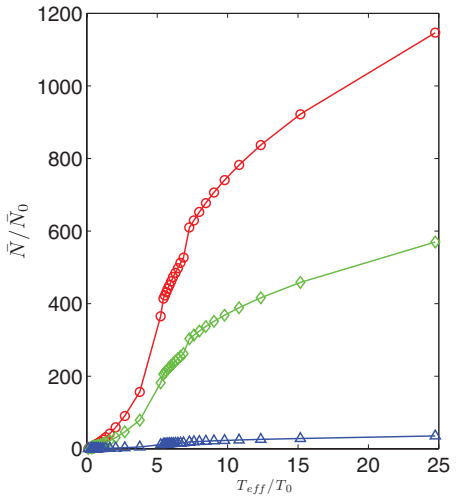

FIG. 6. (Color online) Amplification factor as a function of the effective temperature under different intensities of the external modulation laser. From the top to the bottom: $\gamma\,|\Omega_0|^2/\Delta_0^2 = 1.5\times10^2$, 2×10^2, and 4×10^3, respectively. The other parameters are chosen the same as in Fig. 2.

dipole-dipole interactions) can induce magnon excitations independently. When they take effect simultaneously, the produced magnons from the two channels would interfere with each other, and the constructive interference will take place if the proper parameters are selected.

So far, we have confirmed that the DCE at finite temperature can be observed in our system. This surprising optical phenomenon is simulated by an atomic spin chain confined in an optical lattice, where both the MDDI and the ODDI play an essential role.

IV. DISCUSSION AND CONCLUSIONS

Both short- and long-range spin correlations of atoms in the optical lattice can be probed in the experiments [85,86]. The detection of the spin wave is possible by using optical Raman transitions, where different spin-wave modes can be clearly distinguished. In momentum space, the magnons associated with spin waves of wave number $\mathbf{k}$ have momenta $\mathbf{p} = \hbar k \mathbf{e}_y$. If one observes the Raman scattering using two Raman beams through the Bose gas, the momentum conservation between the magnons and Raman photons requires $\Delta\mathbf{k} = k\mathbf{e}_y$ with $\Delta\mathbf{k}$ being the difference of wave vectors between two Raman beams. Hence, the momentum distribution of the scattered Raman photons can identify the existence of the spin waves with different $\mathbf{k}$, which provides a natural simulation of the DEC at finite temperature.

As proposed in Ref. [87], the squeezing state of the magnon can be excited and detected with magnetic methods [88,89]. Let the ferromagnetic spinor BECs subject to the microwave radiation field $\vec{B} = \hat{\mathbf{x}} B_0 \cos(\omega_B t)$ where B_0 is the amplitude and ω_B is the frequency of the microwave radiation field. The resonance absorption coefficient is proportional to the transition probability:

$$T_{ac} = \frac{\mu_B^2 B_0^2}{\hbar^2} \sum_i \sum_{\mathbf{k}} \int_0^T e^{I\mathbf{k}\cdot\mathbf{R}_i} G_{\mathbf{k}}(t) \cos^2(\omega_B t) dt, \quad (50)$$

where μ_B is the Bohr magneton. From Eq. (50), we can see that T_{ac} will have the minimum value if the magnon squeezing state is achieved. This method can be improved to the time-revolved measurement with high precision [90].

In summary, we have studied the production of the squeezing state of a ferromagnetic magnon and its features in a driven optical lattice. We demonstrated a close analogy of the magnon excitation with the DCE at finite temperature. Our numerical simulations show that the long-range MDDI and ODDI play an important role in this process. In addition to the transverse trapping width and the intensity of the driven laser, many other parameters can be tuned to control the dipole-dipole interactions, for instance, the magnetic field strength, the the laser frequency, and so on. It is expected that the spinor BECs in this system may serve well to simulate more interesting phenomena in condensed matter physics and optical processes.

ACKNOWLEDGMENTS

This work is supported by the National Natural Science Foundation of China under Grants No. 10588402 and No. 11104075, the National Basic Research Program of China (973 Program) under Grant No. 2011CB921600, the Program of Shanghai Subject Chief Scientist under Grant No. 08XD14017, Shanghai Leading Academic Discipline Project under Grant No. B480. The Educational Commission of Henan Province of China under Grant No. 01026631082, and the Postdoctoral Research Foundation of Henan Province under Grant No. 01026500201. L.Z. is supported by the "Chen Guang" project from Shanghai Municipal Education Commission and Shanghai Education Development Foundation under Grant No. 10CG24, and Shanghai Rising-Star Program under Grant No. 12QA1401000.

[1] M. O. Scully and M. S. Zubairy, in *Quantum Optics* (Cambridge University Press, Cambridge, UK, 1997), p. 498.
[2] C. M. Mow-Lowry, B. S. Sheard, M. B. Gray, D. E. McClelland, and S. E. Whitcomb, Phys. Rev. Lett. **92**, 161102 (2004).
[3] J. Estève, C. Gross, A. Weller, S. Giovanazzi, and M. K. Oberthaler, Nature (London) **455**, 1216 (2008).
[4] A. A. Clerk, F. Marquardt, and K. Jacobs, New J. Phys. **10**, 095010 (2008).
[5] J. Grond, U. Hohenester, I. Mazets, and J. Schmiedmayer, New J. Phys. **12**, 065036 (2010).
[6] A. B. Bhattacherjee, J. Phys. B: At., Mol. Opt. Phys. **43**, 205301 (2010).
[7] M. Tsang and C. M. Caves, Phys. Rev. Lett. **105**, 123601 (2010).
[8] W. Heisenberg, Z. Phys. **43**, 172 (1927).
[9] R. E. Slusher, L. W. Hollberg, B. Yurke, J. C. Mertz, and J. F. Valley, Phys. Rev. Lett. **55**, 2409 (1985).
[10] R. Loudon and P. L. Knight, J. Mod. Opt. **34**, 709 (1987).
[11] M. Xiao, L. A. Wu, and H. J. Kimble, Phys. Rev. Lett. **59**, 278 (1987).
[12] L. Davidovich, Rev. Mod. Phys. **68**, 127 (1996).

[13] H. Vahlbruch, S. Chelkowski, K. Danzmann, and R. Schnabel, New J. Phys. **9**, 371 (2007).
[14] C. Marquardt, J. Heersink, R. Dong, M. V. Chekhova, A. B. Klimov, L. L. Sánchez-Soto, U. L. Andersen, and G. Leuchs, Phys. Rev. Lett. **99**, 220401 (2007).
[15] W. N. Plick, J. P. Dowling, and G. S. Agarwal, New J. Phys. **12**, 083014 (2010).
[16] A. Kuzmich, L. Mandel, and N. P. Bigelow, Phys. Rev. Lett. **85**, 1594 (2000).
[17] M. Kitagawa and M. Ueda, Phys. Rev. A **47**, 5138 (1993).
[18] D. J. Wineland, J. J. Bollinger, W. M. Itano, and D. J. Heinzen, Phys. Rev. A **50**, 67 (1994).
[19] J. Hald, J. L. Sørensen, C. Schori, and E. S. Polzik, Phys. Rev. Lett. **83**, 1319 (1999).
[20] B. Julsgaard, A. Kozhekin, and E. S. Polzik, Nature (London) **413**, 400 (2001).
[21] A. Dantan, J. Cviklinski, E. Giacobino, and M. Pinard, Phys. Rev. Lett. **97**, 023605 (2006).
[22] G. R. Jin, Y. C. Liu, and W. M. Liu, New J. Phys. **11**, 073049 (2009).
[23] T. J. Dunn, I. A. Walmsley, and S. Mukamel, Phys. Rev. Lett. **74**, 884 (1995).
[24] M. P. A. Branderhorst, I. A. Walmsley, R. L. Kosut, and H. Rabitz, J. Phys. B: At., Mol. Opt. Phys. **41**, 074004 (2008).
[25] G. Puentes, A. Datta, A. Feito, J. Eisert, M. B. Plenio, and I. A. Walmsley, New J. Phys. **12**, 033042 (2010).
[26] X. Hu and F. Nori, Phys. Rev. Lett. **76**, 2294 (1996).
[27] X. D. Hu and F. Nori, Phys. Rev. B **53**, 2419 (1996).
[28] G. Garrett, J. Whitaker, A. Sood, and R. Merlin, Science **275**, 1638 (1997).
[29] A. Bartels, T. Dekorsy, and H. Kurz, Phys. Rev. Lett. **84**, 2981 (2000).
[30] A. G. Stepanov, J. Hebling, and J. Kuhl, Phys. Rev. B **63**, 104304 (2001).
[31] A. Hussain and S. R. Andrews, Phys. Rev. B **81**, 224304 (2010).
[32] J. F. Wang, Z. Cheng, Y. X. Ping, J. M. Wan, and Y. M. Zhang, Phys. Lett. A **353**, 427 (2006).
[33] Z. Z. Cheng, B. Xu, Z. M. Li, and Z. Cheng, Eur. Phys. J. B **66**, 289 (2008).
[34] F. Peng, Europhys. Lett. **54**, 688 (2001).
[35] J. M. Zhao, A. V. Bragas, D. J. Lockwood, and R. Merlin, Phys. Rev. Lett. **93**, 107203 (2004).
[36] J. Zhao, A. V. Bragas, R. Merlin, and D. J. Lockwood, Phys. Rev. B **73**, 184434 (2006).
[37] V. N. Gridnev, Phys. Rev. B **77**, 094426 (2008).
[38] H. Pu, W. P. Zhang, and P. Meystre, Phys. Rev. Lett. **87**, 140405 (2001).
[39] Kevin Gross, Chris P. Search, Han Pu, Weiping Zhang, and Pierre Meystre, Phys. Rev. A **66**, 033603 (2002).
[40] W. Zhang, H. Pu, C. Search, and P. Meystre, Phys. Rev. Lett. **88**, 060401 (2002).
[41] X. D. Zhao, Z. W. Xie, and W. P. Zhang, Phys. Rev. B **76**, 214408 (2007).
[42] X. D. Zhao, Z. W. Xie, and W. P. Zhang, Acta Phys. Sin. **56**, 6358 (2007).
[43] V. V. Dodonov, A. B. Klimov, and D. E. Nikonov, J. Math. Phys. **34**, 2742 (1993).
[44] R. Golestanian and M. Kardar, Phys. Rev. Lett. **78**, 3421 (1997).
[45] M. Kardar and R. Golestanian, Rev. Mod. Phys. **71**, 1233 (1999).
[46] F. Chen, U. Mohideen, G. L. Klimchitskaya, and V. M. Mostepanenko, Phys. Rev. Lett. **88**, 101801 (2002).
[47] T. Emig, Europhys. Lett. **62**, 466 (2003).
[48] H. Gies and K. Klingmüller, Phys. Rev. Lett. **97**, 220405 (2006).
[49] A. Agnesi *et al.*, J. Phys.: Conf. Ser. **161**, 012028 (2009).
[50] G. L. Klimchitskaya, U. Mohideen, and V. M. Mostepanenko, Rev. Mod. Phys. **81**, 1827 (2009).
[51] V. V. Dodonov, Phys. Scr. **82**, 038105 (2010).
[52] A. V. Dodonov and V. V. Dodonov, Phys. Rev. A **86**, 015801 (2012).
[53] A. V. Dodonov and V. V. Dodonov, Phys. Rev. A **85**, 063804 (2012).
[54] A. V. Dodonov and V. V. Dodonov, Phys. Rev. A **85**, 055805 (2012).
[55] Farid Khelili, Phys. Rev. D **85**, 125013 (2012).
[56] G. Vacanti, S. Pugnetti, N. Didier, M. Paternostro, G. M. Palma, R. Fazio, and V. Vedral, Phys. Rev. Lett. **108**, 093603 (2012).
[57] C. M. Wilson, G. Johansson, A. Pourkabirian, J. R. Johansson, T. Duty, F. Nori, and P. Delsing, Nature (London) **479**, 376 (2011).
[58] G. Plunien, R. Schützhold, and G. Soff, Phys. Rev. Lett. **84**, 1882 (2000).
[59] G. Schaller, R. Schützhold, G. Plunien, and G. Soff, Phys. Rev. A **66**, 023812 (2002).
[60] Y. N. Srivastava, A. Widom, S. Sivasubramanian, and M. P. Ganesh, Phys. Rev. A **74**, 032101 (2006).
[61] V. A. Yampolskii, S. Savelev, Z. A. Mayselis, S. S. Apostolov, and F. Nori, Phys. Rev. Lett. **101**, 096803 (2008).
[62] D. T. Alves, E. R. Granhen, H. O. Silva, and M. G. Lima, Phys. Rev. D **81**, 025016 (2010).
[63] César, D. Fosco, Fernando C. Lombardo, and Francisco D. Mazzitelli, Phys. Rev. D **86**, 045021 (2012).
[64] H. Jing, Q. Y. Shi, and J. S. Wu, Phys. Lett. A **268**, 174 (2000).
[65] H. Saito and H. Hyuga, Phys. Rev. A **78**, 033605 (2008).
[66] T. Akatsuka, M. Takamoto, and H. Katori, Nat. Phys. **4**, 954 (2008).
[67] T. L. Ho, Phys. Rev. Lett. **81**, 742 (1998).
[68] T. Ohmi and K. Machida, J. Phys. Soc. Jpn **67**, 1882 (1998).
[69] C. K. Law, H. Pu, and N. P. Bigelow, Phys. Rev. Lett. **81**, 5257 (1998).
[70] S. Yi, O. E. Mustecaplioglu, C. P. Sun, and L. You, Phys. Rev. A **66**, 011601 (2002).
[71] H.-Y. Lu, H. Lu, J.-N. Zhang, R.-Z. Qiu, H. Pu, and S. Yi, Phys. Rev. A **82**, 023622 (2010).
[72] L. Santos, G. V. Shlyapnikov, P. Zoller, and M. Lewenstein, Phys. Rev. Lett. **85**, 1791 (2000).
[73] S. Yi, L. You, and H. Pu, Phys. Rev. Lett. **93**, 040403 (2004).
[74] S. Yi, O. E. Mustecaplioglu, and L. You, Phys. Rev. Lett. **90**, 140404 (2003).
[75] S. Yi, T. Li, and C. P. Sun, Phys. Rev. Lett. **98**, 260405 (2007).
[76] S. Yi and H. Pu, Phys. Rev. Lett. **97**, 020401 (2006).
[77] T. Holstein and H. Primakoff, Phys. Rev. **58**, 1098 (1940).
[78] C. J. Pethick and H. Smith, in *Bose-Einstein Condensation in Dilute Gases* (Cambridge University Press, Cambridge, 2002), p. 207.
[79] C. M. Caves and B. L. Schumaker, Phys. Rev. A **31**, 3068 (1985).
[80] B. L. Schumaker and C. M. Caves, Phys. Rev. A **31**, 3093 (1985).
[81] L. Mandel, Opt. Lett. **4**, 205 (1979).

[82] W. Nolting and W. D. Brewer, in *Fundamentals of Many-Body Physics: Principles and Methods* (Springer, Berlin, 2009), p. 97.
[83] T. Nikuni, M. Oshikawa, A. Oosawa, and H. Tanaka, Phys. Rev. Lett. **84**, 5868 (2000).
[84] S. O. Demokritov, V. E. Demidov, O. Dzyapko, G. A. Melkov, A. A. Serga, B. Hillebrands, and A. N. Slavin, Nature (London) **443**, 430 (2006).
[85] K. G. L. Pedersen, B. M. Andersen, G. M. Bruun, O. F. Syljuasen, and A. S. Sorensen, Phys. Rev. A **84**, 041603(R) (2011).
[86] Inés de Vega, J. Ignacio Cirac, and D. Porras, Phys. Rev. A **77**, 051804(R) (2008).
[87] F. Peng, Phys. B (Amsterdam) **334**, 183 (2003).
[88] M.-S. Chang, C. D. Hamley, M. D. Barrett, J. A. Sauer, K. M. Fortier, W. Zhang, L. You, and M. S. Chapman, Phys. Rev. Lett. **92**, 140403 (2004).
[89] B. Y. Ning, S. Yi, Jun Zhuang, J. Q. You, and Wenxian Zhang, Phys. Rev. A **85**, 053646 (2012).
[90] C. Kittel, *Introduction to Solid State Physics* (Wiley, New York, 1976), Chap. 16.